

EFFECTS OF GEOMETRIC TOLERANCE IN FLUID DYNAMICS

Lucia Parussini*, Valentino Pediroda[†] and Carlo Poloni^{††}

Department of Mechanical Engineering
University of Trieste
Via Valerio 10, 34127 - Trieste (TS), ITALY
e-mail: *lparussini@units.it [†]pediroda@units.it ^{††}poloni@units.it

Key words: Fluid Dynamics, geometric uncertainties, Tensorial-expanded Chaos Collocation method, Fictitious Domain method, Spectral hp Element method

Abstract. *In this work an approach is presented for the analysis of the effects of geometric tolerances in fluid dynamic behaviour of manufactured components. The Tensorial-expanded Chaos Collocation method coupled to Fictitious Domain Method has been used to solve Fluid Dynamic problems with geometric uncertainties. The main advantage of the Tensorial-expanded Chaos Collocation method is its non-intrusive formulation, so existing deterministic solvers can be used. The Least-Squares Spectral Element Method has been employed for the analysis of the deterministic differential problems obtained by Tensorial-expanded Chaos Collocation. This algorithm exploits a Fictitious Domain approach, so it is particularly suitable to solve differential problems defined on stochastic domains. The capabilities of the Tensorial-expanded Chaos Collocation method combined to the Fictitious Domain-Least-Squares Spectral Element Method are demonstrated by a numerical experiment.*

1 INTRODUCTION

In the engineering design phase of a component tolerance specifications are provided and, since geometric tolerances can influence the performance of the component, an analysis on the way this affects its behavior should be performed. Moreover the sensitivity of the performances respect to the geometric uncertainties should be investigated. Therefore there is a great interest in developing a methodology to face differential problems where the geometrical domain is treated as a stochastic phenomenon.

To introduce the concept of geometric uncertainty, let us consider a one-dimensional model problem:

$$\frac{d^2\phi}{dx^2} = 0 \quad \text{in } [0, L]$$

with $\phi(0) = \phi_0$, $\phi(L) = \phi_L$ and $L = N(L_{Mean}, \sigma_L)$ (1)

where ϕ_0 and ϕ_L are constants and L is a random parameter with Gaussian distribution.

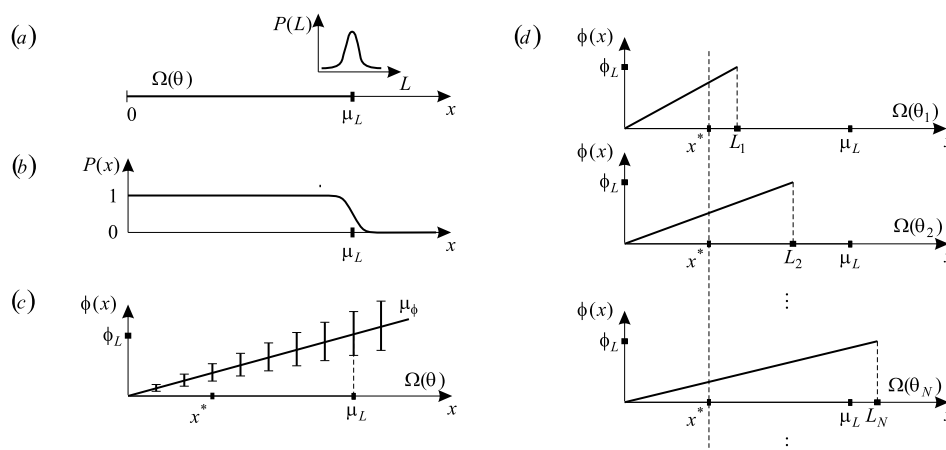


Figure 1: (a) Representation of the stochastic domain of the problem Eq.(1) with normal distribution of length L . (b) Probability $P(x)$ of a point of belonging to domain $\Omega(\theta)$. (c) Representation of the stochastic solution $\phi(x, \theta)$ of problem Eq.(1): the mean value μ_ϕ and the uncertainty bars $\mu_\phi \pm \sigma_\phi$ are shown, referring to absolute coordinates. (d) Representation of different deterministic solutions $\phi(x)$ corresponding to different domains $\Omega(\theta_i)$ of the problem Eq.(1).

In figure 1(a) the stochastic domain of the problem Eq. (1) is shown. The geometric uncertainty, due to the probabilistic distribution $P(L)$ of domain length L , is an uncertainty on the position of boundary condition. A deterministic solution in the domain $\Omega(\theta_i)$ corresponds to each length of domain L_i with probability $P(L_i)$ (see figure 1(d)). So, given $P(L)$, the probability distribution of the stochastic solution $\phi(x^*, \theta)$ can be computed by all the possible deterministic solutions in the point x^* , using a methodology for the un-

certainty quantification. It follows the solution of the problem, shown in figure 1(c), has a probability distribution $P(\phi)$ associated to each point of domain in absolute coordinates.

Obviously the points have not the same probability to belong to the domain. In figure 1(b) the probability $P(x)$ of a point of belonging to domain, which depends on the probabilistic distribution of L , is shown for the problem Eq. (1).

According to this concept of geometric uncertainty, we avoid the mapping of the stochastic domain onto a deterministic domain as in Ref. [1] and every point of the domain is studied in absolute coordinates.

Now to solve a differential problem with geometric uncertainties, Polynomial Chaos methodologies can be used. If the Chaos Polynomial method is employed, we have to solve a set of coupled differential problems, whereas if the Chaos Collocation method is used, we have to solve a set of decoupled differential problems defined in deterministic domains.

Here a Chaos Collocation methodology coupled to a Fictitious Domain solver is used. The basic idea is to avoid the mapping of the stochastic domain onto a deterministic domain referring the stochastic solution to absolute coordinates and at the same time to avoid the remeshing of domain geometry exploiting the Fictitious Domain approach.

In the Fictitious Domain method, problems formulated on a complex domain can be solved on a simple-shaped Fictitious Domain containing the original one. In this way the computational domain of state problem, i.e. the Fictitious Domain, is not influenced by small variations of the original domain boundaries subject to the uncertainty, which are now immersed into the computational domain. Being the computational domain independent by random geometric parameters, the remeshing has not to be performed when the domain geometry changes.

Here, we employ the Tensorial-expanded Chaos Collocation method with the Fictitious Domain-Least Squares Spectral Element Method [2] to solve stochastic Fluid Dynamic problems. The CFD problems under study is the flow past a backward-facing step with perpendicularity tolerance on the step.

2 UNCERTAINTY QUANTIFICATION: TENSORIAL-EXPANDED CHAOS COLLOCATION METHOD

In this work we use a non-intrusive methodology, the Tensorial-expanded Chaos Collocation method (**TeCC**), for the description of stochastic phenomena, whose capabilities have been demonstrated in Ref. [2].

For introducing this uncertainty quantification method, let us consider the following stochastic differential equation:

$$L(\mathbf{x}, t, \theta; \phi) = f(\mathbf{x}, t, \theta) \quad (2)$$

where L is a differential operator which contains space and time differentiation and can be non linear and dependent on random parameters θ ; $\phi(\mathbf{x}, t, \theta)$ is the solution and function

of the space $\mathbf{x} \in \mathfrak{R}^d$, time t and random parameters θ ; $f(\mathbf{x}, t, \theta)$ is a space, time and random parameters dependent source term.

Substituting the Polynomial Chaos series (see Ref.s [3, 4, 5, 6]), given by

$$\begin{aligned} \phi(\mathbf{x}, t, \theta) &= \sum_{i=0}^N \phi_i(\mathbf{x}, t) \Psi_i(\boldsymbol{\xi}) \\ &= \sum_{p_1=0}^{P_1} \sum_{p_2=0}^{P_2} \dots \sum_{p_n=0}^{P_n} \phi_{p_1 p_2 \dots p_n}(\mathbf{x}, t) H_{p_1}(\xi_1) H_{p_2}(\xi_2) \dots H_{p_n}(\xi_n) \end{aligned} \quad (3)$$

for Gaussian random inputs, where $H_{p_k}(\xi_k)$ is the Hermite polynomial of order p_k in terms of the k -th random variable ξ_k with Gaussian distribution $N(0, 1)$, into the stochastic differential Eq. (2) we obtain:

$$L \left(\mathbf{x}, t, \theta; \sum_{i=0}^N \phi_i(\mathbf{x}, t) \Psi_i(\boldsymbol{\xi}(\theta)) \right) \cong f(\mathbf{x}, t, \theta). \quad (4)$$

The method of Weighted Residuals is adopted to solve this equation. The coefficients $\phi_i(\mathbf{x}, t)$ are obtained imposing the inner product of the residual with respect to a weight function equal to zero.

The Collocation method is obtained using a Dirac delta function as weight function. Using a collocation projection on both sides of Eq. (4), we obtain:

$$L(\mathbf{x}, t, \theta_j; \phi_j) = f(\mathbf{x}, t, \theta_j) \quad j = 0, \dots, N. \quad (5)$$

This formulation is a linear system equivalent to the solution of a deterministic problem at each collocation point, called *Chaos Collocation* [7, 8]. If in Eq. (4) the spectral representation is based on the tensorial product of one-dimensional orthogonal polynomials, as that defined in Eq. (3) for Gaussian random variables, the Chaos Collocation approach will be referred as the *Tensorial-expanded Chaos Collocation* method [2]. So that the collocation points are unambiguously defined and they are the Gauss quadrature points of the polynomial with order $P_k + 1$ in each dimension.

Solving the linear system Eq. (5) we obtain the coefficients $\phi_i(\mathbf{x}, t)$ of the spectral expansion and the expected value and the variance of the stochastic solution $\phi(\mathbf{x}, t, \theta)$ will be:

$$E_{PC}(\phi) = \mu_\phi = \phi_0(\mathbf{x}, t) \quad (6)$$

$$Var_{PC}(\phi) = \sigma_\phi^2 = \sum_{i=1}^N [\phi_i^2(\mathbf{x}, t) \langle \Psi_i^2 \rangle]. \quad (7)$$

with $\langle \cdot, \cdot \rangle$ inner product.

Once the stochastic solution is obtained a sensitivity analysis can be easily performed to understand how the problem is affected by the uncertain input parameters and their

respective influence. In most practical problems, we are interested not only in stochastic solution of the problem, but also how the solution changes when the parameters of the problem change. There are several possible procedures to perform the sensitivity analysis [9]. The local methods [10] are based on the first-order approximation of function $\phi(\mathbf{x}, t, \theta)$, which takes the form:

$$\phi(\mathbf{x}, t, \theta) = \phi(\mathbf{x}, t, \theta_0) + \left. \frac{\partial \phi(\mathbf{x}, t, \theta)}{\partial \theta} \right|_{\theta=\theta_0} (\theta - \theta_0). \quad (8)$$

We define the first-order sensitivity coefficient of the function ϕ to the uncertain parameter variation as

$$S_{\theta_0}^{\phi} = \left. \frac{\partial \phi(\mathbf{x}, t, \theta)}{\partial \theta} \right|_{\theta=\theta_0} \quad (9)$$

and θ_0 is the nominal parameter value for which the sensitivity analysis is performed.

Sensitivity analysis is very useful to investigate the robustness of the results respect to the input variables and to identify what source of uncertainty weights more on the solution. Sensitivity analysis has the role of ordering by importance the strength and relevance of the input parameters in determining the variation in the output and in models involving many input variables sensitivity analysis is an essential ingredient.

3 FICTITIOUS DOMAIN - LEAST SQUARES SPECTRAL ELEMENT METHOD

If we have to compute the mean and standard deviation of an analytical function, the implementation of TeCC methodology is quite simple, but in Fluid Dynamic problems we compute the mean and standard deviation of solutions of differential equations. It appears clear that, if we can not solve analytically the differential equation, we have to remesh the computational domain for each new simulation and it is well-known that to find an appropriate parameterization of partitions of domain, which is good for all geometries, is a difficult task for two- or three-dimensional problems.

To overcome this problem we introduce the Fictitious Domain methodology and exploit it to solve differential problems with uncertain parameters. In this way the stochastic domain does not coincide with the computational domain, which is the same for all simulations (Fig. 2) and therefore only the trace of Lagrange multipliers has to be modified in order to enforce the immersed boundary conditions defining the geometry.

The approach we use in this work is the coupling of Fictitious Domain according to Boundary Lagrangian approach [11] together with the Least Squares Spectral Element Method (LSqSEM) [12].

Let us consider the stationary Navier-Stokes equations governing the incompressible flow, which in dimensionless form can be stated as follows:

$$(\mathbf{u} \cdot \nabla) \mathbf{u} + \nabla p + \frac{1}{Re} \nabla \cdot [(\nabla \mathbf{u}) + (\nabla \mathbf{u})^T] = \mathbf{f} \quad \text{in } \Omega \quad (10)$$

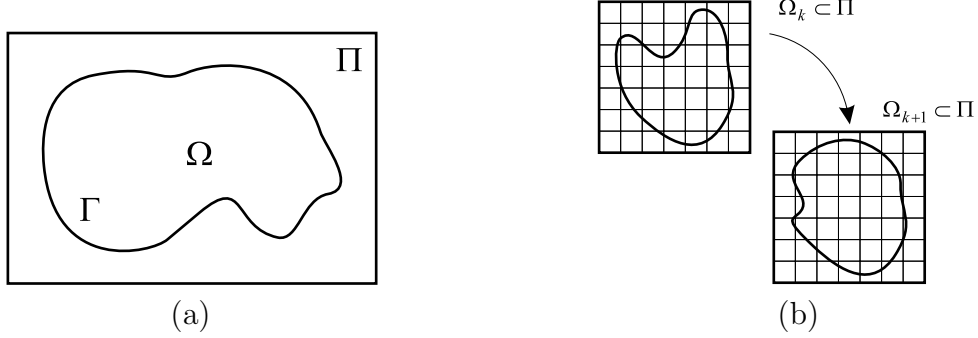


Figure 2: (a) Example of a fictitious rectangular domain Π containing the original domain Ω . (b) Representation of Fictitious Domain approach to solve differential problems defined on a domain which changes in time and space.

$$\nabla \cdot \mathbf{u} = 0 \quad \text{in } \Omega \quad (11)$$

$$\mathbf{u} = \mathbf{u}^s \quad \text{on } \Gamma_u \quad (12)$$

$$\boldsymbol{\sigma} \cdot \hat{\mathbf{n}} = \mathbf{f}^s \quad \text{on } \Gamma_f \quad (13)$$

where $\Gamma = \Gamma_u \cup \Gamma_f$ and $\Gamma_u \cap \Gamma_f = \emptyset$, Re is the Reynolds number, \mathbf{u} is the velocity vector, p is the pressure, \mathbf{f} is a dimensionless force, $\boldsymbol{\sigma} = -p\mathbf{I} + 1/Re [(\nabla\mathbf{u}) + (\nabla\mathbf{u})^T]$, $\hat{\mathbf{n}}$ is the outward unit normal on the boundary of Ω , \mathbf{u}^s is the prescribed velocity on the boundary Γ_u and \mathbf{f}^s are the prescribed tractions on the boundary Γ_f . We assume that the problem is well posed and that a unique solution exists.

To implement the Fictitious Domain theory we extend the L^2 least squares functional for Navier-Stokes equations associated with its vorticity based first-order equivalent system to the simple shaped domain $\Pi \supset \Omega$ and enforce the immersed boundary conditions along Γ by Lagrange multipliers λ .

The resulting Lagrangian $\mathcal{L} : \mathbf{X} \times M \rightarrow \Re$ writes:

$$\begin{aligned} \mathcal{L}(\mathbf{u}, p, \boldsymbol{\omega}, \lambda; \mathbf{f}) = & \\ & \frac{1}{2} \left(\left\| (\mathbf{u} \cdot \nabla) \mathbf{u} + \nabla p + \frac{1}{Re} \nabla \times \boldsymbol{\omega} - \mathbf{f} \right\|_{0,\Pi}^2 + \|\boldsymbol{\omega} - \nabla \times \mathbf{u}\|_{0,\Pi}^2 + \|\nabla \cdot \mathbf{u}\|_{0,\Pi}^2 \right) + \\ & \langle \lambda (\mathbf{u} - \mathbf{u}^s) \rangle_{0,\Gamma_u} + \langle \lambda (\boldsymbol{\sigma} \cdot \hat{\mathbf{n}} - \mathbf{f}^s) \rangle_{0,\Gamma_f} \quad (14) \end{aligned}$$

where we use the spaces

$$\mathbf{X} = \{(\mathbf{u}, p, \boldsymbol{\omega}) \in \mathbf{H}^1(\Pi) \times H^1(\Pi) \times \mathbf{H}^1(\Pi)\}$$

and

$$M = \{\lambda \in H^{-1/2}(\Gamma)\}.$$

To find the minimum of Lagrangian \mathcal{L} we have to solve the corresponding saddle-point problem. The solution of problem, Eq. (10)-(13), will be the restriction to Ω of the minimum of Lagrangian function Eq. (14).

To get the approximated solution of the minimization problem of least squares functional the spectral hp element method [13, 14, 15, 16] is used. So that the saddle point problem is discretized and a system of equations is generated for the modal unknown coefficients associated with velocity, pressure, vorticity and Lagrange multipliers. Once the discrete problem is obtained, it is linearized by Newton's method [17].

Let us remark that the choice of Lagrange multipliers discrete space is not independent of the discrete spaces of variables \mathbf{u} , p and $\boldsymbol{\omega}$. To ensure the convergence of the solution of discretized model to that one of the continuous problem, the Ladyzhenskaja-Babuska-Brezzi (LBB)-condition, also known as inf-sup condition, has to be satisfied [18, 19].

4 APPLICATION: BACKWARD-FACING STEP WITH GEOMETRIC TOLERANCES

We want to examine the flow past a backward-facing step with geometric tolerances of perpendicularity on the step.

The FD-LSqSEM model for the solution of the deterministic problems generated by the TeCC implementation has been validated in Ref.[20], where the two-dimensional steady flow over a backward-facing step at $Re = 800$ has been considered. The basic flow situation is shown in Fig. 3. In Ref. [20] the obtained results have been compared with those ones tabulated from the benchmark solutions of Ref.s [21, 22, 23, 24, 25] and an excellent agreement has been found.

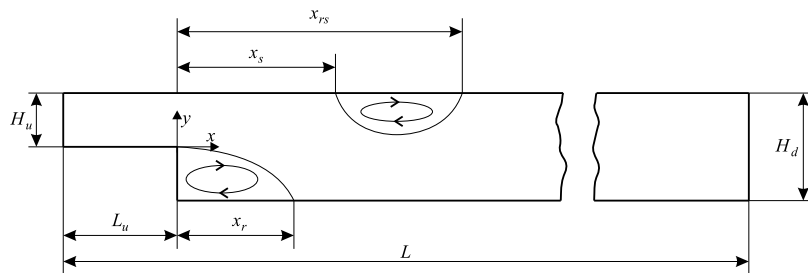


Figure 3: Schematic illustration of flow over a backward-facing step: geometry of flow field.

As the capabilities of the FD-LSqSEM have been demonstrated, let us examine by the integrated approach TeCC and FD-LSqSEM the flow past a backward-facing step with geometric tolerances of perpendicularity on the step (see Fig. 4).

The geometry dimensions, the boundary conditions and the connected model used to solve the deterministic problems are the same used for the validation of FD-LSqSEM solver in Ref.[20].

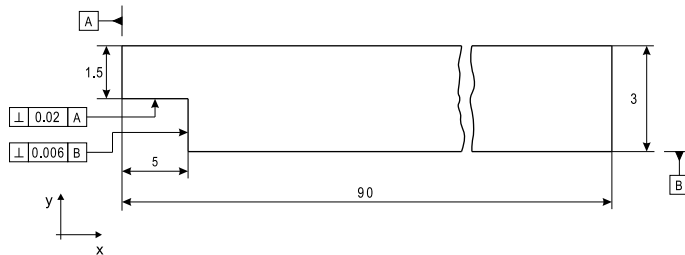


Figure 4: Stochastic flow over a backward-facing step at $Re = 600$: geometric uncertainties.

The geometry and boundary conditions have been taken from the solution of Lee and Mateescu [21]. The expansion ratio H_d/H_u tested is 2.0. The origin of the coordinate system is centered at the step corner. H_u is equal to 1.5 and L_u , the length of the upstream channel, is equal to 5.0. The total length of the channel L is 95.0. The flow is characterized by a Reynolds number $Re = UH_d/\nu$ where U is the average cross-section velocity and ν the kinematic viscosity.

The fictitious domain, $\Pi = [-5.0, 90.0] \times [-1.5, 1.5]$, has been discretized using sixty-three finite elements. The connected model, Π^h , is shown in Fig. 5. The immersed boundary Γ , where no-slip conditions are enforced, has been discretized into four linear finite elements. An 11th order modal expansion has been used in each element of fictitious domain and a 5th order modal expansion in each element of immersed boundary.

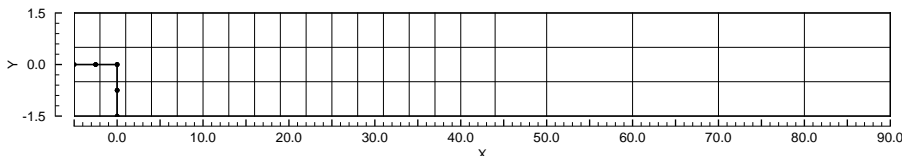


Figure 5: Computational domain and mesh for flow over a backward-facing step: connected model. The reference system is such that $x : y = 1 : 4$.

The resulting discrete model is linearized using Newton’s method. Non-linear convergence is declared when the relative norm of the residuals in velocities, $\|\Delta \mathbf{u}^{hp}\| / \|\mathbf{u}^{hp}\|$, is less than 10^{-4} .

The uncertain parameters are the angle of vertical wall of the step respect to the wall of the channel ($\theta_v = N(0, 0.08)$) and the angle of horizontal wall of the step respect to the inlet section ($\theta_h = N(0, 0.08)$). In practice this spawns the uncertainties on the coordinates of the step corner point.

The flow has been analyzed at Reynolds number $Re = 600$, in fact it has been noticed that because of the presence of geometric tolerances the flow becomes unsteady at $Re = 800$. The analysis starts with $Re = 100$ and steps to $Re = 600$ using a solution continuation technique with increments of $Re = 100$.

The expansion polynomial order of TeCC has been chosen equal to 3, which requires the solution of 16 deterministic decoupled problems.

Fig. 6 shows the field of mean of velocity module V and Fig. 7 the field of its standard deviation. The flow separates from the lower wall after the step and there is a recirculation zone in the upper flow, too. After that, the flow becomes fully developed. The dimensionless length of reattachment on the lower wall of the mean velocity is $x_r = 5.30$, the dimensionless length of separation on the upper wall is $x_s = 4.65$ and the dimensionless length of reattachment on the upper wall is $x_{r_s} = 8.03$. The standard deviation of velocity is higher in correspondence of the geometric uncertainties and it is low in correspondence of the points of reattachment and separation, whereas the height of separation zones is more influenced by uncertainty.

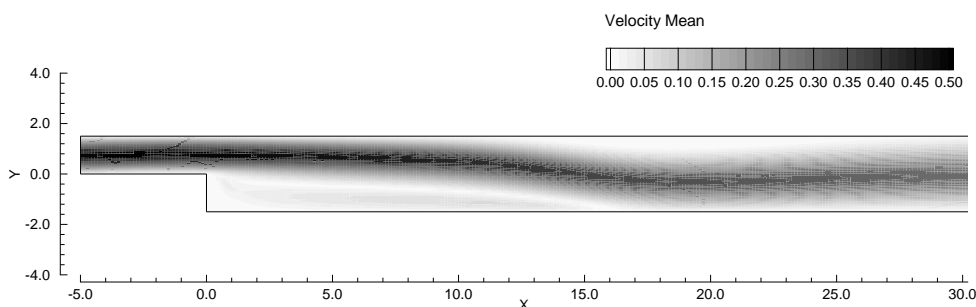


Figure 6: Stochastic flow over a backward-facing step at $Re = 600$: the mean field of the vector velocity.

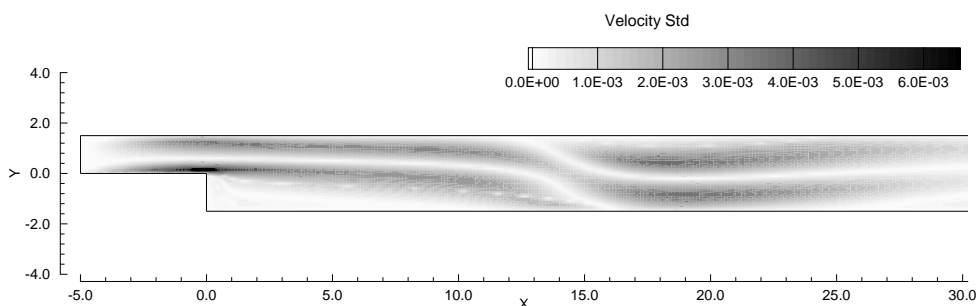


Figure 7: Stochastic flow over a backward-facing step at $Re = 600$: the standard deviation field of the vector velocity.

In Fig. 8 there are the contours of mean of pressure p and in Fig. 9 the contours of its standard deviation. It can be noticed the standard deviation of both velocity and

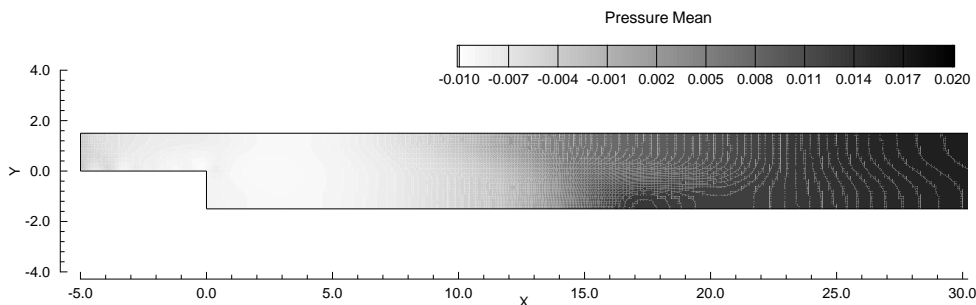


Figure 8: Stochastic flow over a backward-facing step at $Re = 600$: the mean field of the pressure.

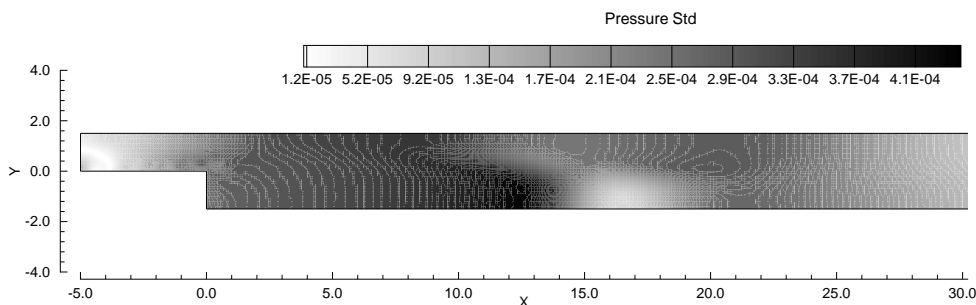


Figure 9: Stochastic flow over a backward-facing step at $Re = 600$: the standard deviation field of the pressure.

pressure is low in correspondence of the reattachment on the lower wall and the standard deviation of pressure increases immediately before the reattachment on the lower wall and on the upper wall.

In Fig. 10 horizontal velocity profiles along the height of the channel at $x = 21$ and $x = 45$ are shown. Both the mean value and the standard deviation are plotted. As we move away from the geometric uncertainties the standard deviation of flow decreases.

The first-order sensitivity coefficients of velocity and pressure respect to the uncertain parameters have been computed. The absolute value of the coefficients, calculated in the mean values of the uncertain parameters, are shown in Figs. 11 and 12. These plots highlight that the flow is more influenced by the angle of horizontal step wall.

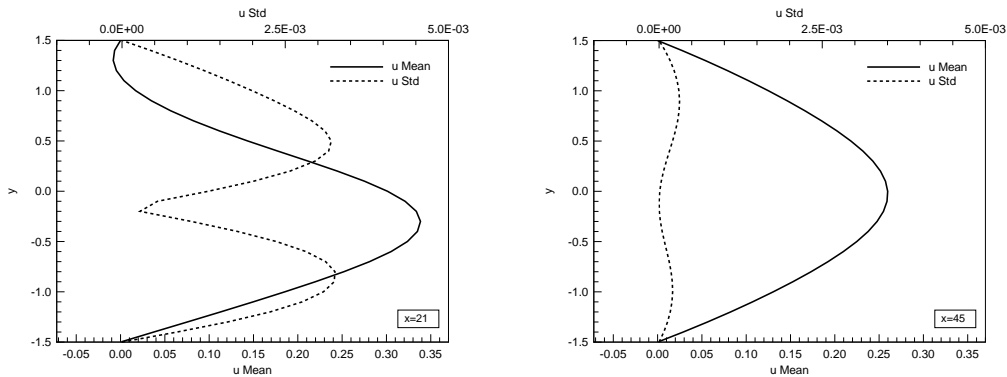


Figure 10: Stochastic flow over a backward-facing step at $Re = 600$: horizontal velocity profiles along the height of the channel at $x = 21$ and $x = 45$. The mean value and the standard deviation are shown.

5 CONCLUSIONS

In this work the Tensorial-expanded Chaos Collocation methodology coupled to a Fictitious Domain solver has been illustrated, in order to solve multi uncertain fluid dynamic problems.

The Fictitious Domain solver we used is based on Least-Squares Spectral Element method. This formulation is of particular interest to study problems defined in stochastic domains, since the Fictitious Domain approach allows avoiding the remeshing of computational domain in the presence of geometric uncertainties. At the same time the exploiting of an higher order discretization method ensures the accuracy of solution.

This paper represents an advanced work in the uncertainty analysis field, both for the theoretical and applicative contents. The approach, which is used for the solution of problems with geometric tolerances, is a novelty in Fluid Dynamics and it promises to have interesting applications in the future.

REFERENCES

- [1] D. Xiu and D. M. Tartakovsky, Numerical methods for differential equations in random domains, *SIAM J. Sci. Comput.*, **28** (3), 1167–1185, (2006).
- [2] L. Parussini and V. Pediroda, Investigation of Multi Geometric Uncertainties by Different Polynomial Chaos Methodologies Using a Fictitious Domain Solver, *CMES Computer Modeling in Engineering & Sciences*, **23** (1), 29–52 (2008).
- [3] N. Wiener, The homogeneous chaos, *Am J Math*, **60**, 897-936 (1938).
- [4] N. Wiener, Nonlinear problems in random theory, *New York: MIT Technology Press and John Wiley and Sons* (1958).

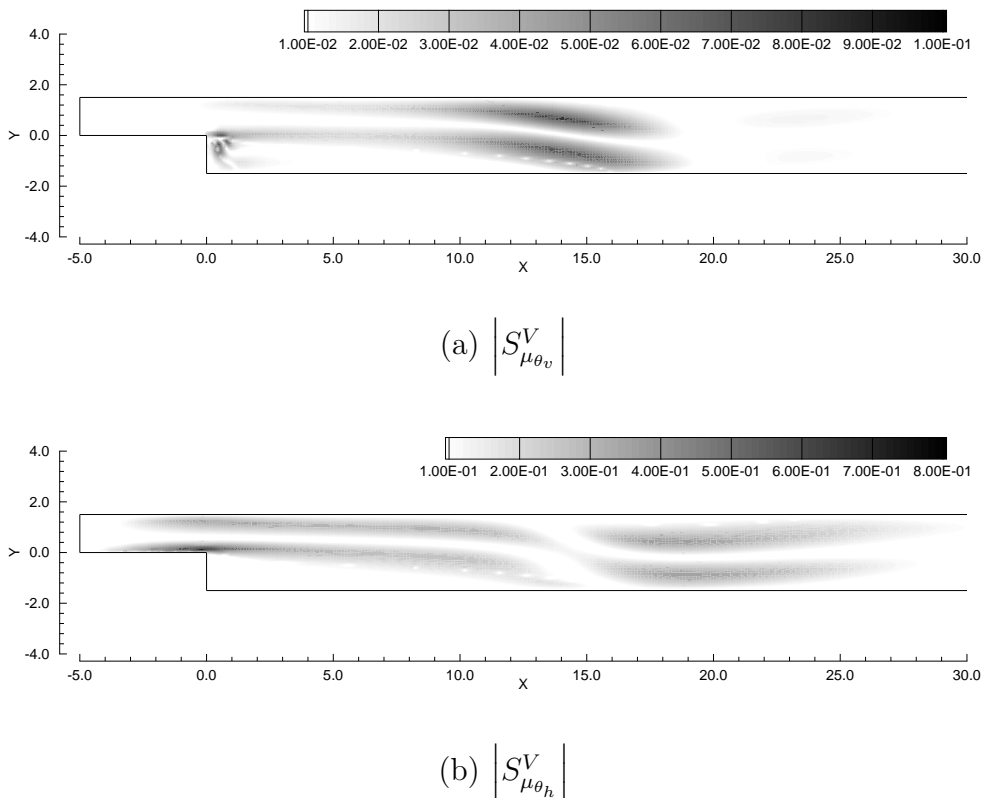


Figure 11: Stochastic flow over a backward-facing step at $Re = 600$: absolute value of the first-order sensitivity analysis coefficient of velocity respect to (a) the angle of vertical wall of the step and (b) the angle of horizontal wall of the step.

- [5] W. Schoutens, Stochastic processes and orthogonal polynomial, *Springer*, 5 edn. (2000).
- [6] A. Askey and J.A. Wilson, Some basic hypergeometric orthogonal polynomials that generalize Jacobi polynomials, *Mem Am Math Soc*, 319.
- [7] G. Loeven, J. Witteveen and H. Bijl, Probabilistic Collocation: An Efficient Non-Intrusive Approach For Arbitrarily Distributed Parametric Uncertainties, In proceedings of the *45th AIAA Aerospace Science Meeting and Exhibit, 8-11 January 2007*, Reno, Nevada, (2007).
- [8] D. Lucor, J. Meyers and P. Sagaut, Sensitivity analysis of large-eddy simulations to subgrid-scale-model parametric uncertainty using polynomial chaos, *Journal of Fluid Mechanics*, **585**, 255–279 (2007).
- [9] S. S. Rao, Engineering Optimization: theory and practice, *John Wiley & Sons*, New York, Third edn. (1996).

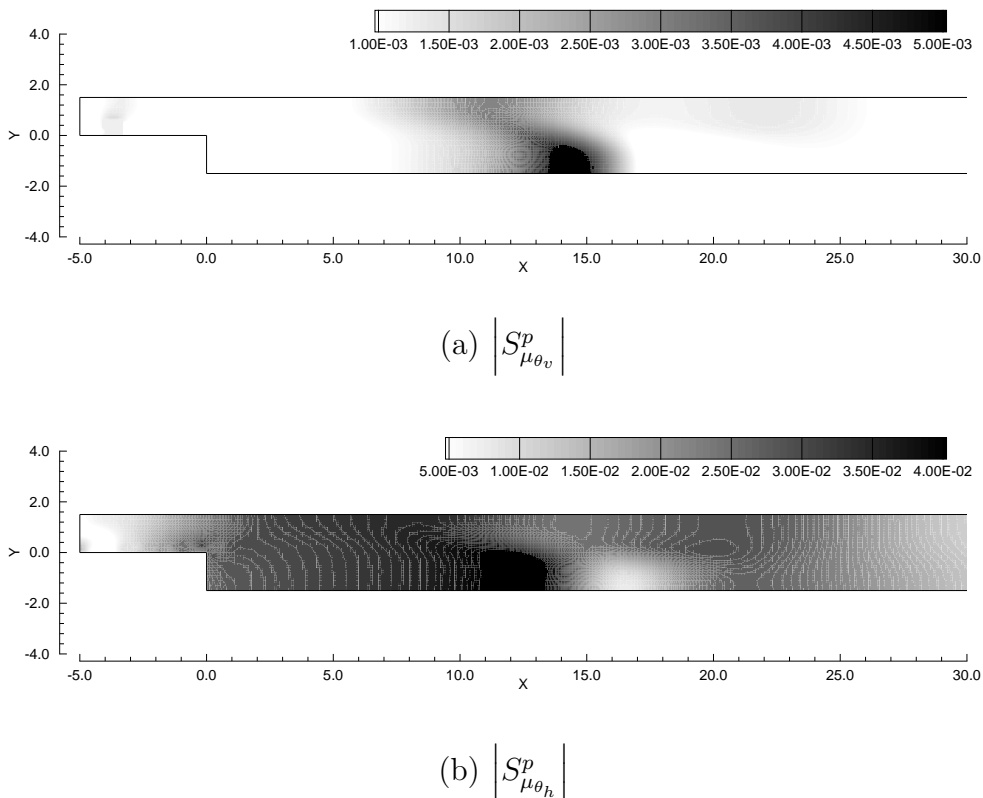


Figure 12: Stochastic flow over a backward-facing step at $Re = 600$: absolute value of the first-order sensitivity analysis coefficient of pressure respect to (a) the angle of vertical wall of the step and (b) the angle of horizontal wall of the step.

- [10] D. G. Cacuci, Sensitivity and Uncertainty Analysis: Theory, Volume I, *Chapman & Hall* (2003).
- [11] I. Babuska, The finite element method with Lagrangian multipliers, *Numer. Math.*, **20**, 179–192 (1973).
- [12] L. Parussini, Fictitious Domain Approach Via Lagrange Multipliers with Least Squares Spectral Element Method, *Journal of Scientific Computing*, **37** (3), 316–335 (2008).
- [13] G. E. Karniadakis and S. J. Sherwin, Spectral/hp Element Methods for CFD, *Oxford University Press*, Oxford (1999).
- [14] M. Gerritsma and B. D. Maerschalck, The least-squares spectral element method, in *VKI Lecture Series 2006-01: 34th CFD - Higher Order Discretization Methods (ISSN : 0377-8312)*, Von Karman Institute, Bruxelles (2006).

- [15] C.-Y. Wu, X.-Y. Liu, A. Scarpas and X.-R. Ge, Spectral Element Approach for Forward Models of 3D Layered Pavement, *CMES Computer Modeling in Engineering & Sciences*, **12** (2), 149–157 (2006).
- [16] D. Komatitsch and J.-P. Vilotte, The spectral element method: an efficient tool to simulate the seismic response of 2D and 3D geological structures, *Bulletin of the Seismological Society of America*, **88**, 368–392 (1998).
- [17] H. Lomax, T. Pulliam and D. Zingg, Fundamentals of computational fluid dynamics, *Springer*, Berlin (2001).
- [18] F. Brezzi and M. Fortin, Mixed and Hybrid Finite Element Methods, Springer Series in Computational Mathematics, Vol.15, *Springer-Verlag* (1991).
- [19] C. Canuto and T. Kozubek, A fictitious domain approach to the numerical solution of PDEs in stochastic domains, *Numerische Mathematik*, **107** (2), 257–293 (2007).
- [20] L. Parussini and V. Pediroda, Fictitious Domain approach with hp-finite element approximation for incompressible fluid flow, *Journal of Computational Physics*, **228**, 3891–3910 (2009).
- [21] T. Lee and D. Mateescu, Experimental and numerical investigation of 2-D backward-facing step flow, *Journal of Fluids and Structures*, **12** (6), 703–716 (1998).
- [22] B. Armaly, F. Durst, J. Pereira and B. Schonung, Experimental and theoretical investigation of backward-facing step flow, *J. Fluid Mech.*, **127**, 473–496 (1983).
- [23] D. K. Gartling, A test problem for outflow boundary conditions - Flow over a backward-facing step, *Int. J. of Numer. Methods in Fluids*, **11**, 953–967 (1990).
- [24] J. Kim and P. Moin, Application of a fractional-step method to incompressible Navier-Stokes equations, *Journal of Comput. Phys.*, **59**, 308–323 (1985).
- [25] J. Sohn, Evaluation of FIDAP on some classical laminar and turbulent benchmarks, *International Journal for Numerical Methods in Fluids*, **8**, 1469–1490 (1988).